NASA TECHNICAL NOTE

NASA TN D-3432

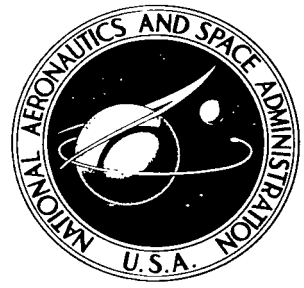

NASA TN D-3432

DETERMINATION OF MEAN ATMOSPHERIC DENSITIES DURING MINIMUM SOLAR ACTIVITY BY MEANS OF THE EXPLORER XIX SATELLITE

by James A. Mullins, Gerald M. Keating, David S. McDougal, and Edwin J. Prior

Langley Research Center
Langley Station, Hampton, Va.

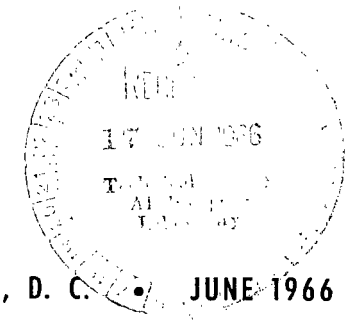

NATIONAL AERONAUTICS AND SPACE ADMINISTRATION • WASHINGTON, D. C. • JUNE 1966

NASA TN D-3432

DETERMINATION OF MEAN ATMOSPHERIC DENSITIES DURING MINIMUM SOLAR ACTIVITY BY MEANS OF THE EXPLORER XIX SATELLITE

By James A. Mullins, Gerald M. Keating, David S. McDougal, and Edwin J. Prior

Langley Research Center
Langley Station, Hampton, Va.

NATIONAL AERONAUTICS AND SPACE ADMINISTRATION

For sale by the Clearinghouse for Federal Scientific and Technical Information
Springfield, Virginia 22151 – Price $1.00

DETERMINATION OF MEAN ATMOSPHERIC DENSITIES DURING MINIMUM SOLAR ACTIVITY BY MEANS OF THE EXPLORER XIX SATELLITE

By James A. Mullins, Gerald M. Keating, David S. McDougal, and Edwin J. Prior
Langley Research Center

SUMMARY

Atmospheric densities are derived from changes in the energy of the Explorer XIX (1963 53A) satellite, a 12-foot-diameter (3.658 m) inflatable sphere. The method of density determination, including the alterations in the method presented in NASA Technical Note D-2895, is described in detail. Because of the low exospheric temperatures experienced by the satellite, the variation of density scale height with altitude is approximately five times as great at perigee altitudes as the values obtained from the U.S. Standard Atmosphere, 1962. Consequently, a more general form of density equation is developed and employed than that used in NASA Technical Note D-2895. The quantities describing the variation of density with altitude – that is, the density scale height and its variation with altitude – are determined from the Jacchia model atmosphere by means of an iteration procedure. A study of the altitude above perigee at which the atmospheric density inferred is least sensitive to the combined uncertainties in density scale height and its variation with altitude resulted in densities being evaluated between $\frac{1}{2}$ and $\frac{\sqrt{3}}{2}$ density scale heights above perigee, depending upon the exospheric temperature. The energy change of the satellite due to solar radiation force is of the same order as that due to drag and, therefore, had to be evaluated.

Equations are given for the solar radiation force on the Explorer XIX and for the aerodynamic drag coefficient as a function of perigee altitude in an atmosphere with low solar heating. Tabulated densities span a period of approximately 7 months before and after the month of minimum solar activity during the present solar cycle, and inferred exospheric temperatures at minimum solar activity were less than 700° K. Also tabulated are: Explorer XIX orbital elements, some parameters useful in analysis of density variations, atmospheric parameters assumed for the calculation of densities, and exospheric temperatures derived from the density points.

INTRODUCTION

The Explorer XIX (1963 53A) satellite is the second in the series of 12-foot-diameter (3.658 m) inflatable spheres which have been placed into orbit solely for the determination of atmospheric densities. The first satellite in this series, Explorer IX (1961 Delta 1), was placed in orbit in February 1961 and reentered the earth atmosphere in April 1964. Explorer XIX was launched late in 1963 so that this series of satellites could continuously sample the density of the atmosphere throughout the 11-year solar cycle and so that atmospheric densities could be obtained simultaneously from two 12-foot-diameter spheres in different portions of the atmosphere.

Atmospheric densities are determined from changes in the orbital elements of the satellite. Since the precision of the densities depends upon the precision of differences in the orbital elements, these low-mass-area-ratio satellites yield more accurate densities than would more compact satellites.

This report is the second in a series of reports on the determination of atmospheric densities from the orbital decay of the 12-foot-diameter spheres and is an extension of the general approach presented in reference 1, a report on the determination of atmospheric densities from the Explorer IX satellite. The method of deriving atmospheric densities is essentially that given in reference 1.

Preliminary density measurements from Explorer XIX indicated an extremely cool atmosphere; a reevaluation of the assumptions of reference 1 was therefore required. The resulting improvements in the method of deriving atmospheric densities include a density equation applicable to a cool atmosphere, the use of a more complex and realistic atmospheric model, a drag coefficient based upon an atmosphere having low solar heating, and a detailed study of the optimum altitude above perigee at which to evaluate the atmospheric density. Also included in the report are a determination of the radiation force upon Explorer XIX and a method of using orbital predictions for density determination.

Atmospheric densities derived from the procedure presented herein are tabulated so that interested parties may analyze them. These densities occur at many positions about the earth since the satellite was in a near-polar orbit and include densities near the North Pole in winter and summer and near the South Pole in spring and fall. The times and positions of the tabulated densities are also given, together with certain parameters related to the given atmospheric models.

SYMBOLS

A frontal area of satellite, 10.51 m^2

$A_2 = Jr_E^2 = 66.0546 \times 10^9$ m^2

a semimajor axis of orbit

$\overline{\Delta a_D}$ change in semimajor axis of orbit per revolution due to aerodynamic drag averaged over many revolutions

b correction factor for deviation of atmosphere from constant H

C_D aerodynamic drag coefficient

$\overline{C_D}$ effective aerodynamic drag coefficient

C_S solar constant at 1 astronomical unit, 1.395342×10^3 $J\text{-}m^{-2}\text{-}sec^{-1}$

c speed of light in a vacuum, 2.99793×10^8 $m\text{-}sec^{-1}$

ΔE_D change in energy of satellite per revolution due to aerodynamic drag

$\overline{\Delta E_D}$ change in energy of satellite per revolution due to aerodynamic drag averaged over many revolutions

e eccentricity of orbit

$\vec{F}_S$ force exerted on satellite by direct solar radiation

H density scale height, $-\frac{\rho}{d\rho/dh}$

h height above earth

i inclination of orbit to equator of date

J coefficient of second harmonic in earth gravitational potential, 1.6236×10^{-3}

K correction factor for rotation of atmosphere

$\vec{L}$	unit vector in direction of solar radiation incident on satellite
M	computed value of mean anomaly
M_A	observed value of mean anomaly
ΔM	observed value minus computed value of mean anomaly
M_0, M_1, M_2	constants associated with mean anomaly
m	satellite mass, 8.069 kg
n	mean (anomalistic) motion
r	distance from center of earth to satellite
r_E	equatorial radius of earth, 6378.388 km
r_S	geocentric distance from earth to sun in astronomical units
r_{sat}	radius of satellite, 1.829 m
$\vec{r}(\phi)$	vectorial reflectance of surface for light incident at angle ϕ
s	ratio of estimated-to-actual density scale height at perigee
T_W	wall temperature of satellite
T_∞	exospheric temperature
t	time
t_E	epoch time
α	right ascension
β	angular velocity of earth rotation, 7.2722052×10^{-5} rad-sec^{-1}
δ	declination

ϵ	eccentric anomaly
$\theta(\phi)$	angle between normal to area element and direction of vectorial reflectance
λ	constant denoting fraction of estimated density scale height above perigee at which density is evaluated
μ	product of universal gravitational constant and mass of earth, 3.9861353×10^{14} m^3-sec^{-2}
ρ	atmospheric density
Φ	term used in evaluation of density at λH^* above perigee
ϕ	angle of incidence of solar radiation
Ω	right ascension of ascending node referred to equinox of 1950.0 and equator of date
ω	argument of perigee

Subscripts:

p	at perigee
p+25	at perigee plus 25 km
p-25	at perigee minus 25 km
p+100	at perigee plus 100 km
$p+\lambda H^*$	at perigee plus λH^*

Superscript:

*	estimated perigee value

A dot over a symbol indicates the derivative with respect to time.

EXPERIMENT DESCRIPTION

Atmospheric drag occurs principally in the vicinity of perigee for moderate orbital eccentricities because of the rapid decrease of atmospheric density with altitude. Then, by measuring drag perturbations, densities in the vicinity of perigee can be deduced.

The Explorer XIX (1963 53A) satellite with its extremely low mass-area ratio (0.7680 kg-m^{-2}) was placed into a moderately eccentric orbit (0.114) so that atmospheric densities could be accurately determined from satellite energy decay and so that the position of the density measurement could be determined. A near-polar orbit (inclination of 78.6^{o}) was chosen so that, as the perigee point precessed, densities could be sampled from both polar and equatorial latitudes.

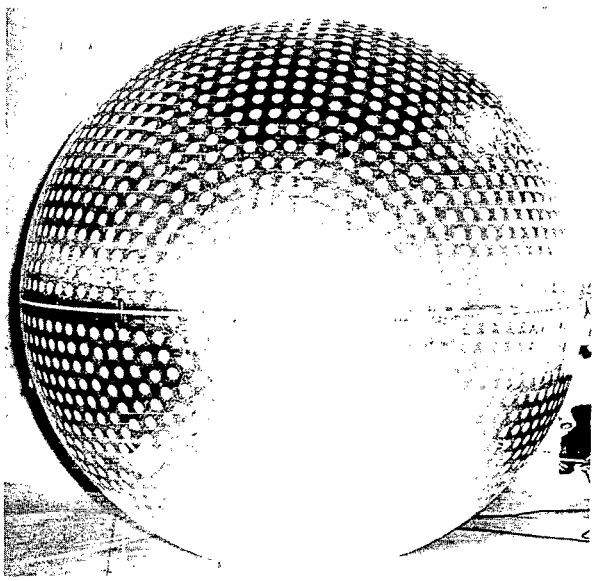

Figure 1.- Explorer XIX satellite. L-64-9380

Figure 1 is a photograph of the Explorer XIX satellite, a spherical balloon which has a diameter of 12.0 feet (3.658 m) and a mass of 8.069 kg (ref. 2). The satellite is constructed of a four-ply laminate of alternating layers of aluminum foil and plastic film with the aluminum on the external surface. Uniformly distributed over the surface of the sphere are 2-inch-diameter (5.1 cm) dots of white paint for thermal control. (See ref. 3 for this method of thermal control.) A minitrack beacon is attached to the skin and uses the electrically separated hemispheres of the balloon as an antenna; it is powered by four panels of solar cells situated about the sphere at the apexes of an imaginary equilateral tetrahedron (ref. 2).

Explorer XIX was launched at 18^{h}49^{m} GMT on December 19, 1963, from the Pacific Missile Range into a near-polar orbit. Explorer XIX had an inclination of 78.6^{o}, a perigee height of 592 km, and an apogee height of 2392 km. The orbit is synchronized with the sun so that near-polar densities have always been obtained near midnight local time.

PROCEDURE

The basic procedure used in obtaining atmospheric densities from low-mass-area-ratio satellites, as given in reference 1, is briefly as follows: Observations of the satellite

are collected from various sources. Because of the low output of the radio beacon aboard the satellite, the principal source of observations for the Explorer XIX satellite was the Baker-Nunn photographic network. Orbital elements are obtained as a function of time by using a differential improvement program. In this report, the results of the Smithsonian Astrophysical Observatory Differential Orbit Improvement Program (refs. 4 and 5) have been used. From the time-dependent orbital elements, the total energy decay of the satellite orbit due to perturbing forces is deduced by the method presented in reference 1. The energy changes due to forces other than atmospheric drag are evaluated and the resulting energy changes are subtracted from the total energy decay to yield the energy decay due to atmospheric drag. The mean atmospheric density may then be determined once certain aerodynamic properties of the satellite and certain properties of the atmosphere are assumed.

In the following sections, the alterations of the method of reference 1 are given. Of course, differences in the physical characteristics of Explorer XIX and Explorer IX have made it necessary to obtain new values of the solar radiation force, the coefficient of drag, and the mass-area ratio. The low temperature of the atmosphere required changes in the equation used for density determination and in the assumed density profiles. An improved density equation is presented which is compatible with a new atmospheric model which has a variable exospheric temperature. A study is made of the altitude above perigee at which the density determination is least sensitive to the assumed density profile. Most of the provisional orbital elements used for density determination were obtained for prediction purposes and are consequently referenced to a time after the observations used for their determination. A method of backdating is described by which these elements are improved.

Atmospheric Density at Perigee

The following expression has been developed for the energy decay per revolution due to atmospheric drag acting on a satellite (ref. 1):

$$\Delta E_D = -\frac{\mu A \overline{C_D}}{2} \int_{\epsilon=0}^{\epsilon=2\pi} \frac{(1 + e\cos\epsilon)^{3/2}}{(1 - e\cos\epsilon)^{1/2}} \rho \, d\epsilon \tag{1}$$

Rearranging terms gives the atmospheric density at perigee ρ_p:

$$\rho_p = \frac{-2\Delta E_D}{\mu A \overline{C_D} \int_{\epsilon=0}^{\epsilon=2\pi} \frac{(1 + e\cos\epsilon)^{3/2}}{(1 - e\cos\epsilon)^{1/2}} \left(\frac{\rho}{\rho_p}\right) d\epsilon} \tag{2}$$

where

ΔE_D	change in energy of satellite per revolution due to aerodynamic drag
A	frontal area of satellite
μ	product of universal gravitational constant and mass of earth
$\overline{C_D}$	effective aerodynamic drag coefficient
ρ	atmospheric density
e	eccentricity of orbit
ϵ	eccentric anomaly

If the procedure of reference 6 is used, the atmospheric density is assumed to obey the following equation:

$$\rho = \rho_p \left[1 + b(r - r_p)^2\right] e^{-\frac{(r-r_p)}{Hp}} \tag{3}$$

where H_p defined by

$$H \equiv \frac{-\rho}{d\rho/dh} \tag{4}$$

is the density scale height at perigee, b is a constant associated with the variation of H, r is the distance from the center of the earth to the satellite, and r_p is the distance from the center of the earth to the satellite at perigee.

Upon substitution of equations (3) and (24) into equation (2) and expansion of the integrand in equation (2) as a power series in eccentricity, the integral may be replaced by Bessel functions of imaginary argument which, when in turn are replaced by their asymptotic expansions and terms of order e^3 or higher are dropped, yield the following equation:

$$\rho_p = \frac{-1}{2K\overline{C_D}}\left(\frac{m}{A}\right)\sqrt{\frac{2e}{\pi a H_p}}\left(\frac{\overline{\Delta a_D}}{a}\right)\left[1 + 2e + \frac{3}{2}e^2 + \frac{H_p}{8ae}\left(1 - 6e + \frac{9H_p}{16ae}\right)\right.$$

$$\left. + \frac{3}{4}bH_p^2\left(1 + 2e + \frac{5H_p}{8ae} + \frac{105H_p^2}{128a^2e^2}\right)\right]^{-1} \qquad \left(\frac{3H_p}{a} \leqq e \leqq 0.2\right) \qquad (5)$$

In equation (5), m is the satellite mass, a is the semimajor axis of the orbit, and $\overline{\Delta a_D}$ is the change in the semimajor axis of the orbit per revolution due to atmospheric drag averaged over many revolutions.

The quantity K is a correction factor to account for the satellite velocity relative to an atmosphere rotating with the earth and is given by the following equation:

$$K = \left[1 - \frac{r_p \beta \cos i}{\sqrt{\mu\left(\frac{2}{r_p} - \frac{1}{a}\right)}}\right]^2 \qquad (6)$$

where

β angular velocity of earth rotation

i satellite inclination

Equation (5) is different from the final form given in reference 6. In reference 6, bH_p^2 is assumed to be no greater than 0.05, and the variation of density scale height with altitude is set equal to $2bH_p^2$. An investigation of the atmospheric model in reference 7 shows that bH_p^2 may have values of 0.25 or greater and that the variable slope of the curve of H with altitude is not adequately represented for the present purposes when it is evaluated at perigee. Therefore, equation (5), a more general equation, has been incorporated.

Choice of H_p and b

The choice of values for H_p and b is dependent upon the choice of the atmospheric model. Shown in figure 2 is an atmospheric model of variable exospheric temperature. The exospheric temperature, T_∞ is the temperature which the atmosphere asymptotically approaches with altitude. In figure 2, $\log_{10}$ of atmospheric density (density measured in gram-cm^{-3}) is presented as a function of geometric altitude with exospheric temperature as a parameter. This model, developed by Jacchia (ref. 7), will be, with small alterations, the model incorporated in the U.S. Supplemental Atmospheres, 1966 (not as yet published). Densities obtained from the Explorer XIX satellite correspond to

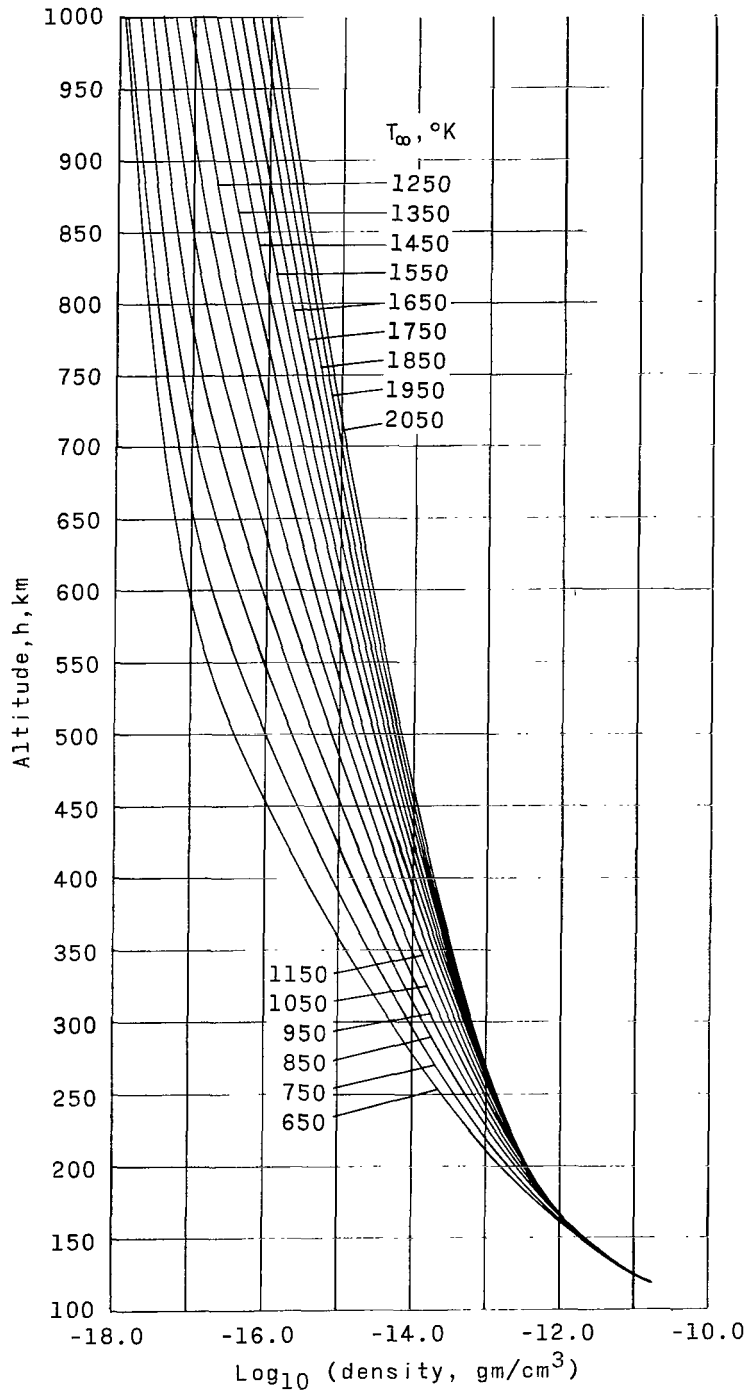

Figure 2.- Jacchia model of $\log_{10}$ density (unit of density is gm/cm^3) as a function of altitude for various exospheric temperatures.

exospheric temperatures below 900° K given in the Jacchia model. These low temperatures are assumed to be due largely to the reduced output of extreme ultraviolet radiation from the sun and the consequent reduced heat input into the atmosphere as the sun approached minimum solar activity in its 11-year solar cycle.

Shown in figure 3 is the density scale height in km, evaluated by using equation (7), as a function of altitude in km for the Jacchia model atmosphere (ref. 7) and the U.S. Standard Atmosphere, 1962 (ref. 8). As may be seen, the values of H at an altitude of 600 km for exospheric temperatures below 900° K differ significantly from that given by the U.S. Standard Atmosphere, 1962. Therefore, the values of H_p and b in this paper were chosen from the Jacchia model of reference 7.

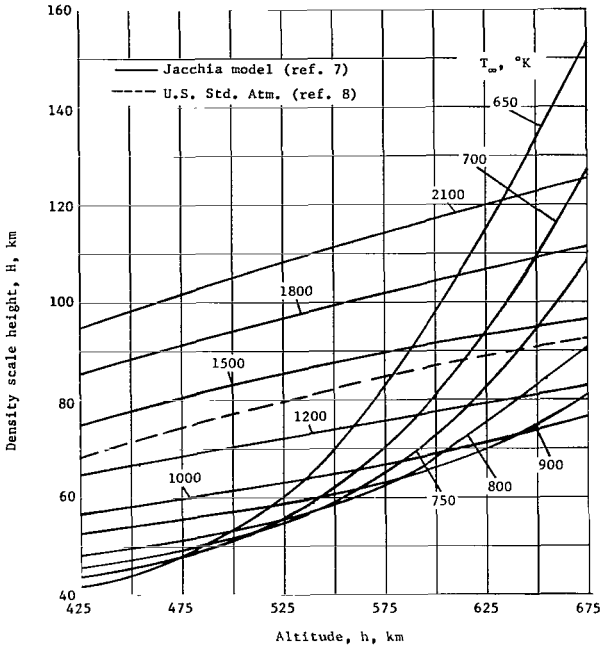

Figure 3.- Density scale height obtained from the U.S. Standard Atmosphere, 1962, and from Jacchia for several exospheric temperatures.

The accuracy of the Jacchia density model is primarily dependent upon the boundary conditions assumed at 120 km and the temperature profiles assumed above this altitude. In order for a density-altitude point to correspond to one temperature, there must be only one density profile for each exospheric temperature. This is probably not the case (ref. 9) during diurnal heating and cooling. But this model atmosphere does seem to best fit density data up to the present time.

Values of H_p and b were chosen so that the variation of density with altitude would adequately fit the density model. The following expressions, derived from equations (4) and (3), were used to evaluate H_p and b:

$$H_p = \frac{r_{p+25} - r_{p-25}}{\ln \rho_{p-25} - \ln \rho_{p+25}} \tag{7}$$

$$b = \frac{\rho_{p+100} - \rho_p \exp\left(\frac{-100}{H_p}\right)}{\left(10^4\right)\rho_p \exp\left(\frac{-100}{H_p}\right)} \tag{8}$$

where H_p is in km.

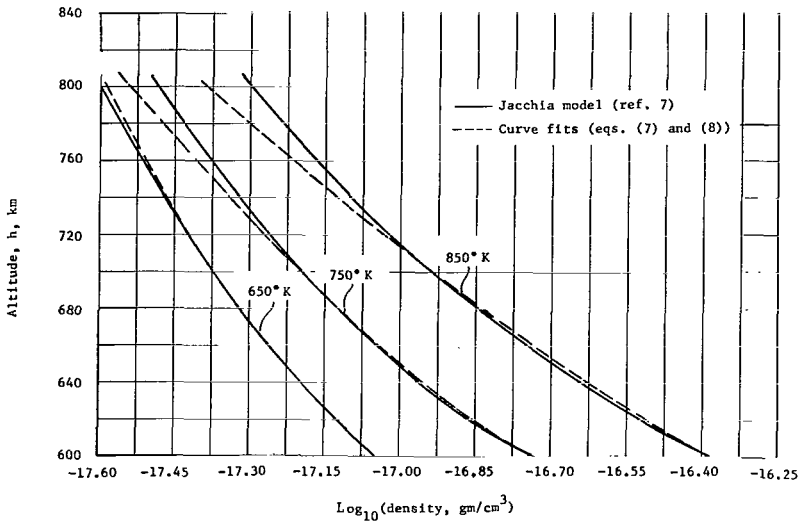

Figure 4.- Comparison of Jacchia model atmosphere with curve fits for low exospheric temperatures.

In figure 4, $\log_{10}$ of density is plotted as a function of altitude for model atmospheres given in reference 7 for exospheric temperatures of 650° K, 750° K, and 850° K. These atmospheres are similar to those experienced by Explorer XIX during this data interval. The densities obtained from reference 7 are shown by the solid-line curves, and those obtained from the calculated values of H_p and b are shown by the dash-line curves. The densities closely match, especially over the first critical 100 km.

In order to evaluate properly H_p and b, the atmosphere of appropriate exospheric temperature must be used. The exospheric temperature is evaluated by an iterative method. Initially, the following expressions are used to obtain rough approximations of H_p (ref. 1) and b:

$$H_p = (-5.994 \times 10^{-5})h_p^2 + 0.1659h_p + 7.1687 \tag{9}$$

$$b = 0 \tag{10}$$

where $200 \leqq h \leqq 800$ km. These expressions are substituted into equation (5) to obtain an atmospheric density at perigee. The corresponding exospheric temperature is then computed by linear interpolation of the tabulated $\log_{10}$ of atmospheric density as a function of altitude and exospheric temperature given in reference 7. By using equations (7) and (8) improved values of H_p and b are obtained for the model atmosphere of given exospheric temperature. These improved values are substituted into equation (5) to obtain an improved density from which a new exospheric temperature is obtained. This process is repeated until the value of $\log_{10}$ of density varies by less than 0.001 from

the previously calculated value. Thus, the best values of H_p and b consistent with the atmospheric model are obtained.

The best values of H_p and b are quickly converged upon because of the slow variation of these quantities with density. For example, a 1000-percent error in density of the atmospheric model may only produce an error on the order of 10 percent in H_p and a 5-percent error in the resulting calculated density.

Evaluation of Density Above Perigee

Although the atmospheric model of reference 7 is a definite improvement over the U.S. Standard Atmosphere, 1962, it still may be significantly in error. In order to insensitize the atmospheric density obtained as much as possible to this error, the density may be evaluated at a height above perigee.

By following the procedure of reference 10, the density at λH^* above perigee, where H^* is the best estimate of H_p and where λ is a constant, is obtained from equation (3):

$$\rho_{p+\lambda H^*} = \rho_p\left[1 + b\,(\lambda H^*)^2\right]\exp\left(\frac{-\lambda H^*}{H_p}\right) \tag{11}$$

For evaluating optimum values of λ, equation (5) may be rearranged as follows:

$$\rho_p = \frac{-1}{2K\overline{C_D}}\left(\frac{m}{A}\right)\left(\frac{\overline{\Delta a_D}}{a}\right)\sqrt{\frac{2e}{\pi a H_p}}\left(\frac{1}{1 + \frac{3}{4}bH_p^2}\right)\left[1 + 2e + \ldots\right]^{-1} \tag{12}$$

Combining equations (11) and (12) gives

$$\rho_{p+\lambda H^*} = \Phi\left(\frac{-1}{2K\overline{C_D}}\right)\left(\frac{m}{A}\right)\left(\frac{\overline{\Delta a_D}}{a}\right)\sqrt{\frac{2e}{\pi a H^*}}\left[1 + 2e + \ldots\right]^{-1} \tag{13}$$

where

$$\Phi = \left[\frac{1 + \lambda^2 s^2\left(bH_p^2\right)}{1 + \frac{3}{4}\left(bH_p^2\right)}\, s^{1/2}\exp(-\lambda s)\right] \tag{14}$$

and

$$s = H^*/H_p \tag{15}$$

From a study of equation (13) which differs from the equation developed in reference 10 in the $\left(1 + \frac{3}{4}bH_p^2\right)$ term, it is seen that s, the uncertainty of H_p, and b appear only in the Φ term. Actually the right-hand bracket has such terms, but they are of order e^2 or greater. Therefore, solely for evaluating the values of λ least sensitive to the atmospheric model – that is, to the values of s and b – equation (13) may be used and specifically the Φ term should be evaluated. Once λ is determined from a study of equation (13), densities can be determined from equations (5) and (11).

In figure 5, $\Phi\sqrt{\lambda}$ is plotted against λs for different values of bH_p^2. For $bH_p^2 = 0$, the parameter is seen to peak at $\lambda s = 0.5$. For higher values of bH_p^2 the parameter peaks at increasing values approaching $\lambda s = 2.5$ asymptotically. All parameters cross at $\lambda s = \frac{\sqrt{3}}{2} = 0.866$.

In order to choose best values of λ, the following procedure is undertaken. The effect of certain magnitude errors in s and b is evaluated for Φ, and the best value of λ is chosen for each combination of errors. Shown in figure 6 plotted against λ is the absolute value of the percent deviation of Φ when $bH_p^2 = 0.10$ and $s = 1.0$ obtained

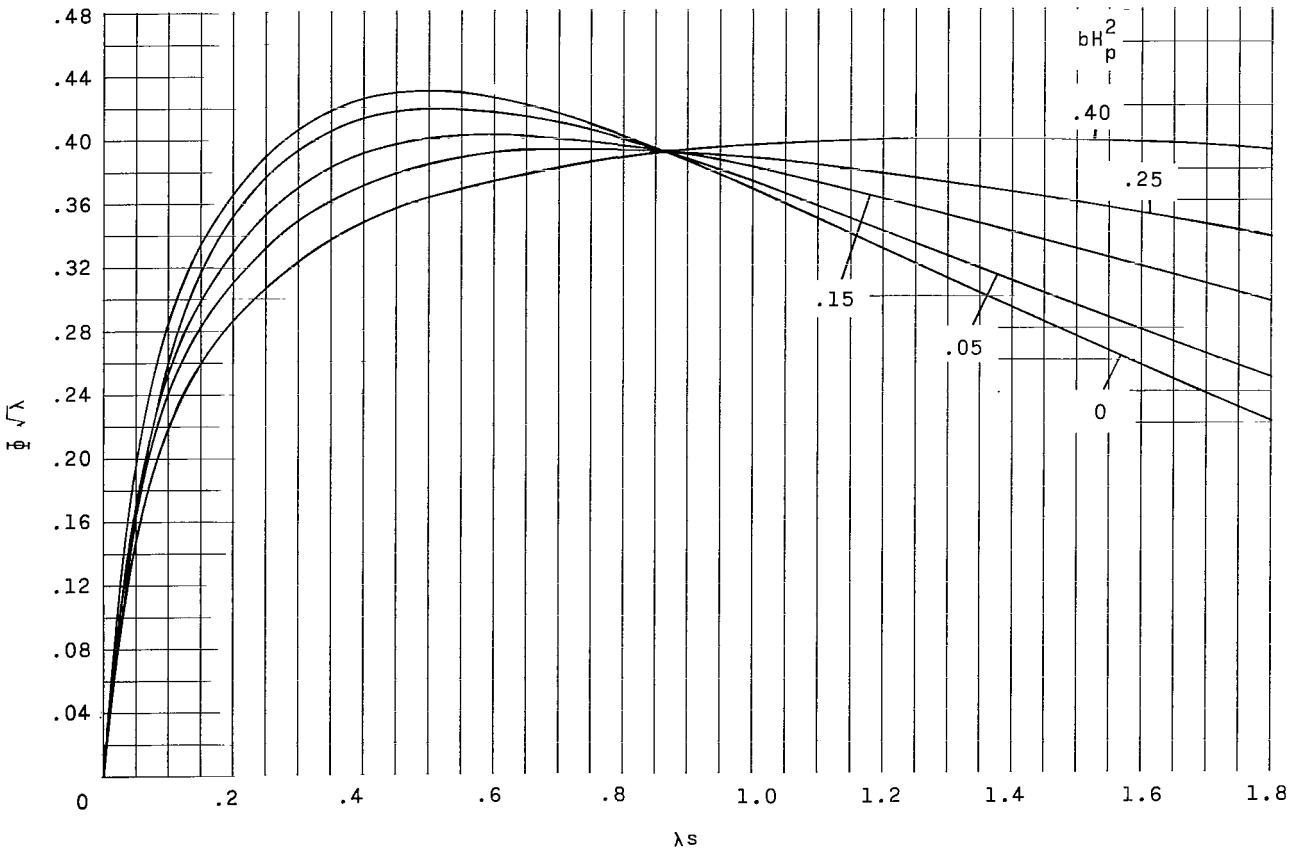

Figure 5.- Variation of $\Phi\sqrt{\lambda}$ with λs for various values of bH_p^2.

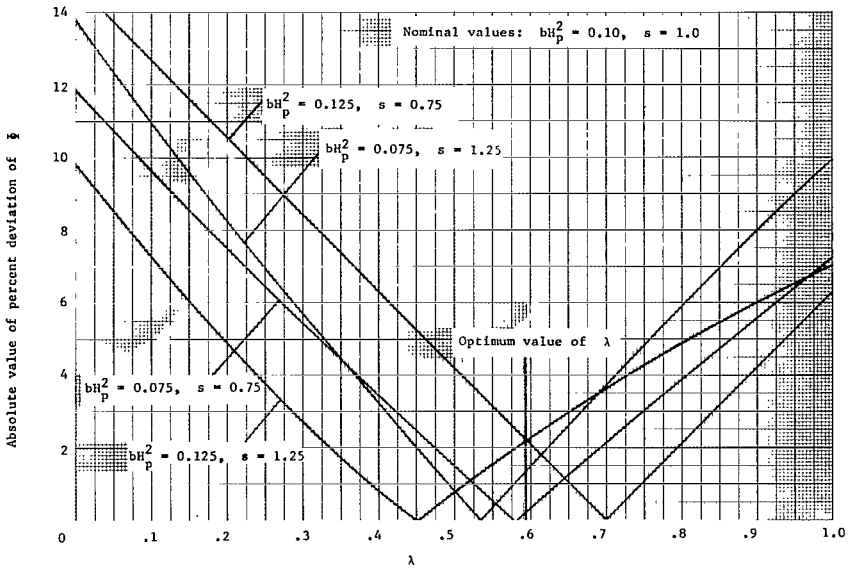

Figure 6.- Method of choosing optimum value of λ for given errors in b and s.

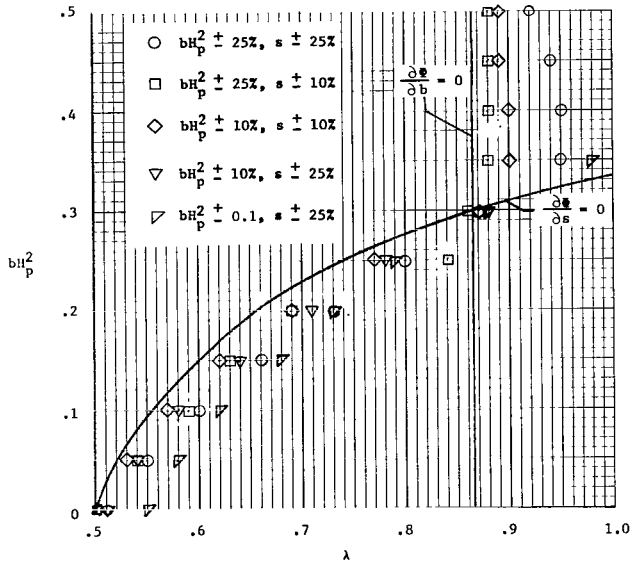

Figure 7.- Optimum values of λ for given errors in b and s.

when errors of ±25 percent are assumed in bH_p^2 and s. The optimum value of λ was chosen where the maximum percent deviation was minimized – that is, at $\lambda = 0.595$. Similar curves were plotted for bH_p^2 between 0 and 0.50.

In figure 7 is plotted the results of the analysis for errors of ±25 percent in bH_p^2 and ±25 percent in s and also the results from the following assumed errors: ±10 percent in bH_p^2 and ±10 percent in s, ±10 percent in bH_p^2 and ±25 percent in s, ±25 percent in bH_p^2 and ±10 percent in s, and finally ±0.1 in bH_p^2 and ±25 percent in s.

Alternatively, the error in Φ may be approximated by

$$\Delta\Phi = \frac{\partial \Phi}{\partial s}\Delta s + \frac{\partial \phi}{\partial b}\Delta b \qquad (16)$$

When $\partial\Phi/\partial s$ is set equal to zero, the following expression is obtained:

$$bH_p^2 = \frac{\left(\lambda s - \frac{1}{2}\right)}{2(\lambda s)^2\left(\frac{5}{4} - \frac{1}{2}\lambda s\right)} \qquad (17)$$

This expression is shown in figure 7 as a solid curve, where s is set equal to 1. In terms of λs, by least mean squares equation (17) may be expressed as

$$\lambda s = 0.500 + 0.588\left(bH_p^2\right) - 1.952\left(bH_p^2\right)^2 + 32.22\left(bH_p^2\right)^3 - 129.6\left(bH_p^2\right)^4 + 227.8\left(bH_p^2\right)^5 \qquad (18)$$

where $0 \leqq bH_p^2 \leqq 0.295$. When $\partial\Phi/\partial b$ is set equal to zero, the following value is obtained independent of b:

$$\lambda s = \frac{\sqrt{3}}{2} \tag{19}$$

Since the actual errors in b and s are unknown and Φ changes slowly with λ, equations (18) and (19) were used to obtain the optimum value of λ. Values of λ were chosen using equation (18) for bH_p^2 between 0.0 and 0.295 and equation (19) for bH_p^2 above 0.295, with s set equal to 1.0.

In order to evaluate the density at λH^* above perigee, the following procedure is incorporated. First, the density at perigee is determined by using equation (5), and by repeated approximations best values of H_p and b are obtained. Then, bH_p^2 is substituted into equation (18) or (19) and the best value of λ is chosen. Finally, ρ_p, bH_p^2, and λ are substituted into equation (11) to obtain the density at the height least sensitive to the density model.

Methods have now been developed for obtaining H_p, b, λ, ρ_p, and $\rho_{p+\lambda H_p}$ once the orbital elements, $\overline{\Delta a_D}$, and $\overline{C_D}$ are known.

Improvement in Orbital Elements

A portion of the mean orbital elements of Explorer XIX made available by Smithsonian Astrophysical Observatory (SAO), which have been used in this report, are unpublished predictions which were originally used by SAO to predict satellite position so that subsequent observations could be made. These orbital elements are obtained from polynomials, with time from epoch as the independent variable, where the epoch time occurs after the observation interval. In order to obtain accurate atmospheric densities, the elements are evaluated at a time during the observation interval. There remains the choice of the optimum time during the observation interval at which the orbital elements should be evaluated.

The atmospheric density is measured from the energy decay of the satellite, which in turn is directly proportional to the time rate of change of semimajor axis, which in turn is proportional to the time rate of change of mean motion. The accuracy of these terms, then, is of prime concern. Slight errors in the other orbital elements have no significant effect on density determination.

The semimajor axis is determined in the SAO Differential Orbit Improvement (DϕI-3) program by the following equation (ref. 4):

$$a = \left(\frac{\mu}{n^2}\right)^{1/3}\left[1 - \frac{A_2}{3a^2}\left(1 - e^2\right)^{-3/2}\left(1 - \frac{3}{2}\sin^2 i\right)\right] \tag{20}$$

where $A_2 = 66.0546 \times 10^9\ m^2$, and n is the mean (anomalistic) motion which is defined as the time rate of change of mean anomaly. The mean anomaly is given in the differential correction program as

$$M = M_0 + M_1(t - t_E) + M_2(t - t_E)^2 \tag{21}$$

where M_0, M_1, and M_2 are constants, t_E is an epoch time, and t is any other time. The equation is most valid over the time interval of observations. Associated with each observation is a residual ΔM giving the difference between the calculated and observed values of mean anomaly. When these residuals are plotted against time, instead of giving random scatter, many times they give a definite trend (fig. 8) indicating that the empirical equation (21) for M may be improved. From the following equation for the observed value of mean anomaly

$$M_A = M_0 + M_1(t - t_E) + M_2(t - t_E)^2 + \Delta M \tag{22}$$

it then follows that

$$n = \dot{M}_A = M_1 + 2M_2(t - t_E) + \dot{\Delta M} \tag{23}$$

The value of $\dot{\Delta M}$ may be found by plotting ΔM as a function of time and taking the slope of a faired curve through the residuals. Equation (21) can then be used for determining n when $\dot{\Delta M} = 0$. Times have been chosen to evaluate n when $\dot{\Delta M} = 0$, and

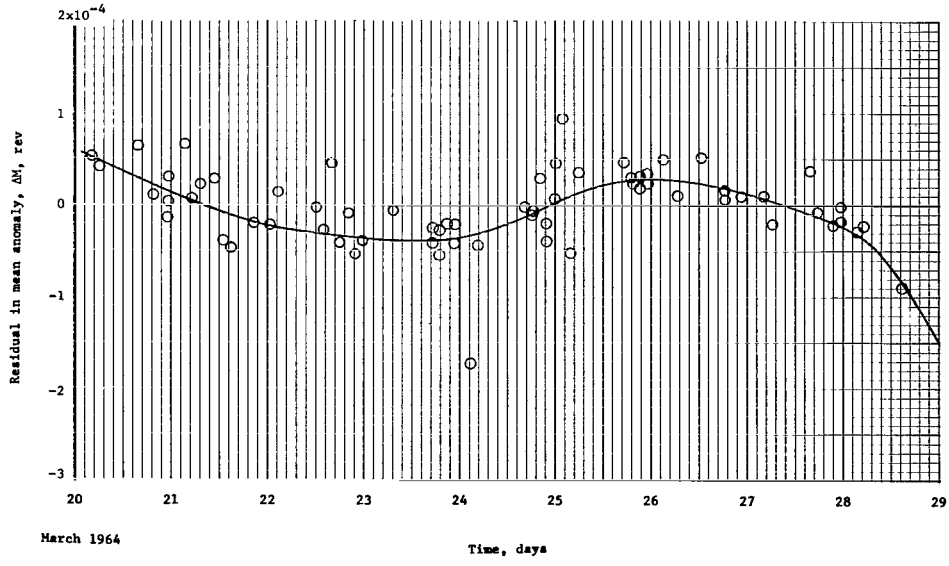

Figure 8.- Residual between observed value and calculated value of mean anomaly.

the constants determined in the differential correction program are most accurate. Once the mean motion n is evaluated, the semimajor axis a may be determined from equation (20). The other orbital elements are then backdated by linear interpolation.

Evaluation of $\overline{\Delta a_D}$

The quantity $\overline{\Delta a_D}$ evaluated by the procedure of reference 1 is given by

$$\overline{\Delta a_D} = \frac{2a^2}{\mu m}\overline{\Delta E_D} \tag{24}$$

where $\overline{\Delta E_D}$ is the energy decay due to atmospheric drag per revolution averaged between successive epochs. This energy decay is evaluated by subtracting the energy decay due to solar radiation force from the total energy decay. The energy decay due to direct solar radiation is directly proportional to the radiation force. The radiation force $\vec{F}_S$ upon Explorer XIX has a different magnitude than the force evaluated on Explorer IX because a larger percent of the surface area of Explorer XIX is covered with white paint and the white paint has a higher reflectivity.

The 12-foot-diameter (3.658 m) Explorer XIX satellite is uniformly covered with 2-inch-diameter (5.1 cm) dots of white paint which constitute 25 percent of its surface area. This silicone paint was found to have a reflectivity of 0.77 to normally incident solar radiation. In comparison, only 18 percent of the Explorer IX surface area was covered by white dots and the white epoxy paint had a reflectivity of 0.70 to solar radiation. Both paints are essentially diffuse reflectors, reflecting light similarly. By using the method of reference 1 and assuming that the vectorial reflectance $\vec{r}(\phi)$ (see ref. 11) for the silicone paint is 77/70 of that for the Explorer IX epoxy paint for all values of ϕ, the radiation force can be expressed as

$$\vec{F}_S = \frac{\pi r_{SAT}^2 C_S}{c r_S^2}\left[1 + 2\left(0.25\left(\frac{77}{70}\right)\int_{\phi=0}^{\phi=\pi/2}\left\{|\vec{r}(\phi)|\cos\left[\phi + \theta(\phi)\right]\right\}_{\substack{\text{white}\\\text{paint}}}\cos\phi\sin\phi\,d\phi\right.\right.$$

$$\left.\left. + 0.75\int_{\phi=0}^{\phi=\pi/2}\left\{|\vec{r}(\phi)|\cos\left[\phi + \theta(\phi)\right]\right\}_{\text{aluminum}}\cos\phi\sin\phi\,d\phi\right)\right]\vec{L} \tag{25}$$

and

$$\vec{F}_S = \frac{\pi r_{SAT}^2 C_S}{c r_S^2}(1.059)\left(\vec{L}\right) \tag{26}$$

Drag Coefficient

The effective drag coefficient $\overline{C_D}$ is defined in reference 1 as

$$\Delta E_D = -\frac{\mu A}{2}\int_{\epsilon=0}^{\epsilon=2\pi}\frac{(1+e\cos\epsilon)^{3/2}}{(1-e\cos\epsilon)^{1/2}}C_D\rho\,d\epsilon = -\frac{\mu A\overline{C_D}}{2}\int_{\epsilon=0}^{\epsilon=2\pi}\frac{(1+e\cos\epsilon)^{3/2}}{(1-e\cos\epsilon)^{1/2}}\rho\,d\epsilon \qquad (27)$$

so that the coefficient of drag may be removed from the integral when the density is being evaluated. An extension of the analysis of reference 1 was undertaken to obtain an expression for the coefficient of drag for the cooler atmosphere experienced by Explorer XIX. At perigee altitudes and velocities the coefficient of drag C_D decreases with increasing eccentricity, whereas above perigee C_D increases with increasing eccentricity. As a result, the effect of increasing eccentricity nearly cancels out for $\overline{C_D}$. If complete thermal accommodation is assumed, $\overline{C_D}$ may be expressed in terms of perigee height h and wall temperature T_w, as follows:

$$\overline{C_D} = 2.037 + 2.54\times10^{-4}(h_p - 500) - 2.7\times10^{-8}(h_p - 500)^2 + \left[0.0058 + 0.164\times10^{-4}(h_p - 500)\right]\sqrt{T}_w \qquad (28)$$

where $500 \leqq h_p \leqq 800$ km. The wall temperature of Explorer XIX varies drastically when it enters and exits the earth's shadow due to the satellite's thermal properties and extremely low mass-area ratio. Wall temperatures of 300° K in sunlight and 175° K in shadow can be expected (ref. 3). With reference to equation (28), this fluctuation in wall temperature will cause a variation of about $\pm 1/2$ percent in $\overline{C_D}$ from a mean value. If a mean wall temperature of 250° K is assumed, the equation for $\overline{C_D}$ used for computation (eq. (28)), reduces to

$$\overline{C_D} = 2.129 + 5.13\times10^{-4}(h_p - 500) - 2.7\times10^{-8}(h_p - 500)^2 \qquad (29)$$

where $500 \leqq h_p \leqq 800$ km. Variation in the kinetic temperature of the air molecules as the perigee approaches the diurnal bulge may cause variations as large as 2 percent from a mean value of $\overline{C_D}$.

ATMOSPHERIC DENSITIES

Presented in table I are mean orbital elements of Explorer XIX derived from mean orbital elements computed by the Smithsonian Astrophysical Observatory using their

Differential Orbit Improvement Program. The more accurate orbital elements have been obtained through March 31, 1964. After that date prediction elements have been improved by backdating. Times were chosen when the time rate of change of residual in mean anomaly was near a minimum. By assuming a linear variation between epochs one week apart, values of eccentricity, argument of perigee, right ascension of ascending node, and inclination were chosen. The value of n was chosen by using the constants associated with mean anomaly determined by the differential correction program. With this method the elements are significantly improved for density determination since they are evaluated at a time during the observation interval instead of being in their original transmitted form – that is, a prediction of the elements after the observation interval.

In the first column in table I, the epoch indicates the reference time for the set of elements. All times are zero Universal Time. The second column gives the mean (anomalistic) motion in revolutions per day. The last four columns give the eccentricity, orbital inclination in degrees, argument of perigee in degrees, and right ascension of the ascending node in degrees. With the exception of the epoch, the last place in each column is unreliable.

With the method described in this paper, mean atmospheric densities and their associated time and position were computed between the successive epochs tabulated in table I. Table II gives the results of these computations. The first four columns are simply midpoints in time, right ascension, declination, and distance from center of earth to satellite at the perigee. The fifth column gives the exospheric temperature in degrees Kelvin, derived from reference 7, corresponding to the altitude and density at $h_p + \lambda H_p$. The values of density scale height H_p, in kilometers, and of b, per km^2, given in columns six and seven, respectively, are derived from the model atmosphere of reference 7 which has the exospheric temperature given in column five. Column eight gives the height of the density point above the international ellipsoid. This height is the perigee height plus λH_p where λ is chosen so that the value of density is least sensitive to the values assumed in columns six and seven or, in other words, least sensitive to the atmospheric model. Column nine gives the $\log_{10}$ of mean atmospheric density at λ scale heights above perigee where density is in $gm\text{-}cm^{-3}$. In the last column is the time interval between successive sets of orbital elements used to infer atmospheric density. As may be seen, the time interval increases from 7 days for the better elements to approximately 14 days for the prediction elements.

Mean exospheric temperatures obtained over the period of study, December 1963 through April 1965, average 820° K with maximum temperatures near 900° K and minimum temperatures of less than 700° K. Minimum temperatures were obtained in July 1964, the month of minimum solar activity over the 11-year solar cycle.

Errors in determination of mean atmospheric density are discussed in reference 1. These errors are attributed to inaccuracies in the determination of energy decay due to drag, aerodynamic drag coefficient, variation of density with altitude, the rate of rotation of the atmosphere, and the assumed atmospheric model. The most significant of these inaccuracies is thought to be the determination of orbital elements from which energy decay is obtained. The optical constraints on tracking by low latitude stations of the near-polar orbit of Explorer XIX has presented periods of the order of 1 month when optical observations could only be collected from one hemisphere. At these times the accuracy of orbit determination has been significantly degraded. More precise laboratory measurements of the tracking photographs may yield higher resolution of atmospheric densities in the future.

CONCLUDING REMARKS

The Explorer XIX (1963 53A) satellite has experienced extremely low atmospheric densities during the first 17 months in orbit, a time of minimum solar activity. The lowest exospheric temperatures inferred from the density measurements with use of the Jacchia model, less than 700° K, were noted during July 1964, the month of minimum solar activity over the 11-year solar cycle.

The variation of density scale height with altitude at 600 km for these low exospheric temperatures is about five times greater than that obtained from the U.S. Standard Atmosphere, 1962. Because of this rapid change of scale height with altitude, a more general form of the density equation than that in NASA Technical Note D-2895 has been developed for density determination.

It was found that the effect on the density determination of the uncertainty of scale height and of its variation with altitude is minimized if densities are evaluated at a height above perigee. This optimum height was found to be between $\frac{1}{2}$ and $\frac{\sqrt{3}}{2}$ scale heights above perigee and is dependent upon the exospheric temperature.

The change in skin temperature when the satellite enters shadow may alter the drag coefficient by one-half of 1 percent, and changes in temperature and composition of the atmosphere as the satellite approaches the diurnal bulge may alter the drag coefficient by 2 percent.

Radiation force effects were of the same order of magnitude as the atmospheric-drag effects and therefore had to be taken into account. The direct solar radiation force

upon Explorer XIX was found to be slightly greater than that upon the similar Explorer IX (1961 Delta 1) because of the difference in the optical properties of the two satellites.

Langley Research Center,
National Aeronautics and Space Administration,
Langley Station, Hampton, Va., January 7, 1966.

REFERENCES

1. Keating, Gerald M.; Mullins, James A.; Coffee, Claude W.; and McDougal, David S.: Determination of Mean Atmospheric Densities From the Explorer IX Satellite. NASA TN D-2895, 1965.

2. Woerner, Charles V.; and Coffee, Claude W., Jr.: Comparison of Ground Tests and Orbital Launch Results for the Explorer IX and Explorer XIX Satellites. NASA TN D-2466, 1964.

3. Woerner, Charles V.; and Keating, Gerald M.: Temperature Control of the Explorer IX Satellite. NASA TN D-1369, 1962.

4. Gaposchkin, E. M.: Differential Orbit Improvement (DØI-3). Spec. Rept. No. 161, Smithsonian Inst. Astrophys. Obs., Aug. 3, 1964.

5. Veis, G.; and Moore, C. H.: Smithsonian Astrophysical Observatory Differential Orbit Improvement Program. Seminar Proceedings – Tracking Programs and Orbit Determination. Astronaut. Inform. (Contract No. NASw-6), Jet Propulsion Lab., California Inst. Technol., c.1960, pp. 165-184.

6. Cook, G. E.; and King-Hele, D. G.: The Contraction of Satellite Orbits Under the Influence of Air Drag. IV. With Scale Height Dependent on Altitude. Proc. Roy. Soc. (London), ser. A, vol. 275, no. 1363, Oct. 29, 1963, pp. 357-390.

7. Jacchia, Luigi G.: Static Diffusion Models of the Upper Atmosphere With Empirical Temperature Profiles. Spec. Rept. No. 170, Smithsonian Inst. Astrophys. Obs., Dec. 30, 1964.

8. Anon.: U.S. Standard Atmosphere, 1962. NASA, U.S. Air Force, and U.S. Weather Bur., Dec. 1962.

9. Harris, Isadore; and Priester, Wolfgang: Time-Dependent Structure of the Upper Atmosphere. NASA TN D-1443, 1962.

10. King-Hele, Desmond: Theory of Satellite Orbits in an Atmosphere. Butterworth, Inc., 1964.

11. Keating, Gerald M.; and Mullins, James A.: Vectorial Reflectance of the Explorer IX Satellite Material. NASA TN D-2388, 1964.

TABLE I.- ORBITAL ELEMENTS OF EXPLORER XIX

Epoch	n, rev/day	e	i, deg	ω, deg	Ω, deg
1963					
Dec. 21.0	12.430120	0.114580	78.592	158.430	76.984
Dec. 28.0	12.430420	.114170	78.620	144.920	70.204
1964					
Jan. 4.0	12.430355	.113800	78.617	131.300	63.447
Jan. 11.0	12.430307	.113390	78.605	117.480	56.701
Jan. 18.0	12.430478	.113070	78.602	103.720	49.948
Jan. 25.0	12.430915	.112852	78.603	89.864	43.194
Feb. 1.0	12.431746	.112837	78.602	75.998	36.439
Feb. 8.0	12.432869	.112950	78.604	62.191	29.685
Feb. 15.0	12.434420	.113300	78.605	48.420	22.929
Feb. 22.0	12.436285	.113480	78.600	34.810	16.162
Feb. 29.0	12.438771	.113300	78.620	21.700	9.410
Mar. 7.0	12.441138	.113630	78.609	7.740	2.621
Mar. 14.0	12.442829	.113370	78.606	354.150	355.844
Mar. 21.0	12.443890	.113020	78.603	340.600	349.065
Mar. 28.0	12.444590	.112420	78.595	326.900	342.295
Apr. 9.5	12.445290	.111250	78.614	302.345	330.170
Apr. 21.5	12.445570	.110420	78.608	278.303	318.570
May 6.5	12.447256	.110210	78.613	248.241	304.049
May 21.5	12.450423	.111280	78.609	218.234	289.526
June 5.5	12.453833	.112240	78.611	189.220	274.989
June 18.5	12.456506	.112730	78.618	163.790	262.381
July 1.5	12.457520	.113900	78.620	138.339	249.772
July 14.5	12.457950	.113210	78.612	113.216	237.158
July 30.5	12.458776	.113440	78.609	82.382	221.631
Aug. 12.5	12.459699	.112690	78.608	56.561	209.048
Aug. 26.5	12.461105	.112830	78.614	29.303	195.474
Sept. 8.5	12.463393	.112670	78.617	4.172	182.858
Sept. 25.5	12.465054	.111440	78.582	331.000	166.394
Oct. 8.5	12.465386	.110600	78.616	305.695	153.736
Oct. 22.5	12.466256	.109450	78.619	277.648	140.150
Nov. 1.5	12.467181	.109230	78.617	257.671	130.449
Nov. 11.5	12.468189	.109290	78.620	237.674	120.751
Nov. 23.5	12.469624	.110030	78.629	214.161	109.104
Dec. 10.5	12.472119	.110290	78.626	180.976	92.607
Dec. 21.5	12.473342	.109260	78.636	158.970	81.926
1965					
Jan. 5.5	12.472895	.109560	78.609	129.949	67.386
Jan. 20.5	12.473222	.108450	78.627	100.506	52.846
Feb. 3.5	12.474556	.108200	78.627	72.627	39.290
Feb. 17.5	12.476942	.108510	78.633	44.904	25.729
Mar. 4.5	12.480618	.108840	78.630	15.726	11.175
Mar. 15.5	12.483231	.108740	78.638	354.177	.491
Apr. 2.5	12.484535	.107180	78.630	318.845	343.013
Apr. 14.5	12.484342	.106390	78.642	295.114	331.349
Apr. 27.5	12.484852	.105150	78.634	268.838	318.741

TABLE II.- MEAN DENSITIES AT λH_p ABOVE PERIGEE, THE TIME AND POSITION OF MEASUREMENT, PROPERTIES OF ASSUMED ATMOSPHERIC MODEL, AND THE TIME INTERVAL OF MEASUREMENT

Epoch	α_p, deg	δ_p, deg	r_p, km	Exospheric temperature, °K	H_p, km	$b \times 10^4$, km^{-2}	$h_p + \lambda H_p$, km	$\log_{10}(\rho, g/cm^3)$	Time interval, days
1963									
Dec. 24.5	247.517	27.721	6972.713	833.9	66.628	0.279	637.634	-16.665	7.0
Dec. 30.5	236.789	40.890	6975.740	812.1	69.089	.311	648.233	-16.795	7.0
1964									
Jan. 7.5	223.981	53.997	6978.831	816.8	70.973	.304	657.627	-16.830	7.0
Jan. 14.5	205.591	66.580	6981.681	822.0	72.471	.298	665.694	-16.854	7.0
Jan. 21.5	167.641	76.756	6983.685	808.1	74.716	.309	672.642	-16.930	7.0
Jan. 28.5	97.706	76.612	6984.365	812.6	74.576	.305	672.964	-16.918	7.0
Feb. 4.5	60.418	66.312	6983.613	809.2	73.904	.309	669.402	-16.911	7.0
Feb. 11.5	42.237	53.706	6981.291	830.2	70.769	.291	659.344	-16.796	7.0
Feb. 18.5	29.503	40.619	6978.566	837.8	68.603	.281	649.596	-16.719	7.0
Feb. 25.5	18.845	27.650	6977.753	893.2	66.737	.214	641.174	-16.492	7.0
Mar. 3.5	8.985	14.424	6976.255	893.5	66.114	.206	635.794	-16.459	7.0
Mar. 10.5	359.419	.926	6975.222	862.8	65.756	.241	633.926	-16.548	7.0
Mar. 17.5	349.919	-12.378	6977.107	842.4	66.496	.269	637.996	-16.639	7.0
Mar. 24.5	340.110	-25.700	6980.515	848.7	67.499	.266	645.172	-16.659	7.0
Apr. 3.2	324.908	-44.250	6987.215	856.5	69.968	.266	660.277	-16.718	12.5
Apr. 15.5	297.154	-66.399	6994.719	815.1	76.943	.298	683.063	-16.957	12.0
Apr. 29.0	190.441	-76.792	6998.620	839.9	76.430	.283	688.031	-16.908	15.0
May 14.0	131.590	-51.750	6994.329	841.5	73.101	.282	673.455	-16.834	15.0
May 29.0	107.215	-23.229	6985.117	795.8	71.079	.327	654.167	-16.878	15.0
June 12.0	87.991	3.429	6978.280	815.4	67.438	.304	639.973	-16.739	13.0
June 26.0	69.846	28.317	6971.067	748.1	71.908	.368	644.275	-16.975	13.0
July 8.0	48.141	52.689	6968.910	680.2	89.532	.324	672.552	-17.248	13.0
July 22.5	354.132	76.226	6970.484	659.4	102.400	.269	696.424	-17.388	16.0
Aug. 6.0	243.151	66.642	6972.202	717.3	83.434	.337	671.634	-17.170	13.0
Aug. 19.5	212.672	41.891	6974.165	751.6	74.311	.355	654.236	-17.011	14.0
Sept. 2.0	192.564	16.399	6973.555	803.6	67.132	.318	637.019	-16.762	13.0
Sept. 17.0	172.133	-12.171	6978.280	801.1	68.124	.323	642.045	-16.798	17.0
Oct. 2.0	150.090	-40.660	6986.041	807.2	72.189	.312	661.383	-16.878	13.0
Oct. 15.5	120.523	-65.654	6993.636	796.6	78.466	.308	684.005	-17.015	14.0
Oct. 27.5	33.576	-78.382	6998.683	805.6	80.130	.297	693.034	-17.029	10.0
Nov. 6.5	331.266	-65.069	6998.949	814.8	78.231	.295	688.146	-16.981	10.0
Nov. 17.5	306.442	-44.764	6995.350	824.4	74.031	.295	673.288	-16.884	12.0
Dec. 2.0	284.431	-17.210	6990.688	841.8	69.451	.279	655.152	-16.736	17.0
Dec. 16.0	265.272	9.831	6993.017	873.7	68.791	.246	654.735	-16.632	11.0
Dec. 29.0	246.636	34.743	6995.739	798.4	75.132	.317	672.141	-16.957	15.0
1965									
Jan. 13.0	217.387	62.480	6998.943	857.1	74.227	.273	682.341	-16.831	15.0
Jan. 27.5	119.142	78.126	7003.974	836.3	78.537	.280	695.528	-16.953	14.0
Feb. 10.5	50.519	56.958	7003.042	832.8	76.890	.287	687.822	-16.928	14.0
Feb. 25.0	25.027	29.660	6999.396	859.2	71.457	.266	668.489	-16.753	15.0
Mar. 10.0	6.811	4.854	6997.318	887.5	69.259	.232	658.541	-16.609	11.0
Mar. 24.5	346.855	-23.007	7003.102	845.3	72.499	.279	671.606	-16.813	18.0
Apr. 8.5	322.512	-51.559	7012.118	819.6	80.658	.286	698.903	-17.015	12.0
Apr. 21.0	282.145	-73.553	7020.026	852.7	81.717	.265	713.178	-16.985	13.0

"The aeronautical and space activities of the United States shall be conducted so as to contribute . . . to the expansion of human knowledge of phenomena in the atmosphere and space. The Administration shall provide for the widest practicable and appropriate dissemination of information concerning its activities and the results thereof."

—NATIONAL AERONAUTICS AND SPACE ACT OF 1958

NASA SCIENTIFIC AND TECHNICAL PUBLICATIONS

TECHNICAL REPORTS: Scientific and technical information considered important, complete, and a lasting contribution to existing knowledge.

TECHNICAL NOTES: Information less broad in scope but nevertheless of importance as a contribution to existing knowledge.

TECHNICAL MEMORANDUMS: Information receiving limited distribution because of preliminary data, security classification, or other reasons.

CONTRACTOR REPORTS: Technical information generated in connection with a NASA contract or grant and released under NASA auspices.

TECHNICAL TRANSLATIONS: Information published in a foreign language considered to merit NASA distribution in English.

TECHNICAL REPRINTS: Information derived from NASA activities and initially published in the form of journal articles.

SPECIAL PUBLICATIONS: Information derived from or of value to NASA activities but not necessarily reporting the results of individual NASA-programmed scientific efforts. Publications include conference proceedings, monographs, data compilations, handbooks, sourcebooks, and special bibliographies.

Details on the availability of these publications may be obtained from:

SCIENTIFIC AND TECHNICAL INFORMATION DIVISION

NATIONAL AERONAUTICS AND SPACE ADMINISTRATION

Washington, D.C. 20546